

# The contribution of the Unresolved Extragalactic Radio Sources to the Brightness Temperature of the sky

M. Gervasi<sup>1,2</sup>, A. Tartari, M. Zannoni<sup>1</sup>, G. Boella<sup>2</sup>, and G. Sironi<sup>1</sup>

*Physics Department, University of Milano Bicocca, Piazza della Scienza 3, 20126 Milano  
Italy*

mario.zannoni@mib.infn.it

## ABSTRACT

The contribution of the Unresolved Extragalactic Radio Sources to the diffuse brightness of the sky was evaluated using the source number - flux measurements available in literature. We first optimized the fitting function of the data based on number counts distribution. We then computed the brightness temperature at various frequencies from 151 MHz to 8440 MHz and derived its spectral dependence. As expected the frequency dependence can be described by a power law with a spectral index  $\gamma \simeq -2.7$ , in agreement with the flux emitted by the *steep spectrum* sources. The contribution of *flat spectrum* sources becomes relevant at frequencies above several GHz. Using the data available in literature we improved our knowledge of the brightness of the unresolved extragalactic radio sources. The results obtained have general validity and they can be used to disentangle the various contributions of the sky brightness and to evaluate the CMB temperature.

*Subject headings:* cosmology: diffuse radiation, radio continuum: galaxies, galaxies: statistics

## 1. Introduction

In the past years measurements of the absolute sky emission at frequency  $\nu \sim 1$  GHz have been carried out to evaluate the brightness temperature ( $T_{cmb}$ ) of the Cosmic Microwave

---

<sup>1</sup>also Italian National Institute for Astrophysics, INAF, Milano.

<sup>2</sup>also Italian National Institute for Nuclear Physics, INFN, Milano-Bicocca.

Background (CMB). Besides the non-trivial problem of assuring an accurate absolute calibration of the measured signal, we need to remember that the sky emission is a superposition of different contributions. After subtracting the local emissions (mainly due to atmosphere inside the main beam, ground and radio frequency interferences in the far side-lobes) the sky brightness temperature ( $T_{sky}$ ) can be written as:

$$T_{sky}(\nu, \alpha, \delta) = T_{cmb}(\nu) + T_{gal}(\nu, \alpha, \delta) + T_{UERS}(\nu) \quad (1)$$

where  $T_{gal}$  is the emission of our galaxy and  $T_{UERS}(\nu)$  the temperature of the unresolved extragalactic radio sources (UERS). In the present paper we evaluate the UERS brightness temperature and its frequency dependence.

This paper follows a series of others describing the measurements of the sky brightness temperature at frequencies close to 1 GHz gathered by the TRIS experiment with an angular resolution  $FWHM_{TRIS} \sim 20$  deg ((Zannoni et al. 2007), (Gervasi et al. 2007), (Tartari et al. 2007)). The results obtained in the present paper were used to disentangle the components of the sky brightness and to evaluate the CMB temperature at the frequencies  $\nu = 600, 820$  and  $2500$  MHz ((Gervasi et al. 2007)). The aim of this work is to provide a new estimate of the integrated contribution of UERS to the diffuse brightness of the sky. An accurate estimate of  $T_{UERS}(\nu)$  is necessary for the TRIS experiment, but also for all the experiments aimed at the study of the spectral distortions in the Rayleigh-Jeans tail of the CMB spectrum. Deviations from the black-body distribution can be present at low frequency, but the amplitude of the distortions at frequencies around 1 GHz is nowadays constrained by past experiments at the level of few tens of mK (Fixen et al. 1996).

Experiments like TRIS (Zannoni et al. 2007) can reach a control of systematics at the level of  $\sim 50$  mK, a remarkable improvement if compared to previous measurements at the same frequencies. On the other hand, relying on the current knowledge of both amplitude and spectrum of the UERS signal (Longair 1966), we can estimate that at 600, 820, 1400 and 2500 MHz (where CMB observations have been carried out in the past) the extra-galactic contribution is respectively  $810 \pm 180$  mK,  $340 \pm 80$  mK,  $79 \pm 19$  mK and  $16 \pm 4$  mK (see for example Sironi et al. (1990)). Using the current 178 MHz normalization (Longair 1966), for state-of-the-art experiments, this means that the uncertainty associated with the UERS at the lowest frequencies (which are the most interesting when looking for CMB spectral distortions), is potentially higher than instrumental systematics. In this paper we show that by exploiting all the data available in literature we can significantly improve the present status of our knowledge about the UERS contribution, and that TRIS-like experiments are essentially limited by the current technology. New and updated estimates of the brightness temperature of UERS will be useful also for feasibility studies of future experiments in this

field.

This paper is organized as follows: Section 2 discusses the general properties of the UERS and the data in literature. In Section 3 we describe the procedure to fit the available number counts; in Section 4 we calculate the UERS sky brightness and its frequency dependence. Finally in Section 5 we discuss the implications of the results obtained for astrophysics and cosmology.

## 2. The extragalactic radio sources

### 2.1. The population of sources

The unresolved extragalactic radio sources contribute as a blend of point sources to the measurements of diffuse emission, especially with poor angular resolution. Actually UERS are an inhomogeneous collection of quasars, radio galaxies, and other objects. These can be both compact and extended sources with different local radio luminosity function, lifetimes and cosmic evolution. An extensive discussion can be found in Longair (1978).

Usually we can distinguish two populations of radio sources: *steep spectrum* sources if  $\alpha > 0.5$ , and *flat spectrum* sources if  $\alpha < 0.5$ , where  $\alpha$  is the spectral index of the source spectrum ( $S(\nu) \propto \nu^{-\alpha}$ ). Compact radio sources, like quasars, have mostly a flat spectrum ( $\alpha \simeq 0$ ) and are most commonly detected at higher frequencies. On the other hand, extended sources like radio-galaxies, have a steep spectrum ( $\alpha \simeq 0.7-0.8$ ) and dominate low frequency counts (see (Peacock & Gull 1981) and (Longair 1978)).

*Steep spectrum* sources and *flat spectrum* sources contribute in different ways to the number counts. *Flat spectrum* sources are important only at high frequency ( $\nu \gtrsim 2$  GHz). In the same range, *flat spectrum* source counts seem to be comparable to *steep spectrum* source counts for high fluxes, but at low fluxes *steep spectrum* sources are still dominating, as shown for example by Condon (1984) and Kellermann & Wall (1987) The total number counts have been successfully fitted using a luminosity evolution model by Peacock & Gull (1981) and Danese et al. (1987).

### 2.2. Isotropy

The large scale isotropy of the extragalactic radio sources has been studied by Webster (1977). He analyzed several samples of sources measured in a cube of 1 Gpc-side, getting an upper limit  $\Delta N/N < 3\%$  on the fluctuation of the source number. This limit is set by the

finite statistics of the sources contained in the survey:  $N \sim 10^4$ .

Franceschini et al. (1989) have evaluated the fluctuation of the source counts assuming a poissonian distribution: at  $\nu = 5$  GHz they found fluctuations of the antenna temperature  $\Delta T_A/T_A < 10^{-4}$  over an angular scale  $\theta \sim 5$  deg. This fluctuation rapidly decreases at larger scales. At lower frequencies the fluctuations increase, but we have at most  $\Delta T_A/T_A < 10^{-2}$  for  $\nu = 408$  MHz and  $\Delta T_A/T_A < 10^{-4}$  for  $\nu = 2.5$  GHz at an angular scale  $\theta \sim 20$  deg.

Due to these considerations, the contribution of UERS to the sky brightness at large angular scale is assumed isotropic in the following discussion. Moreover the radio sources are supposed to be randomly distributed and the fluctuation in the number counts is assumed to be poissonian. A possible anisotropic contribution of UERS is in most cases negligible and limited to the region of the super-galactic plane (see (Shaver & Pierre 1989)).

### 2.3. The data set

Many source-number vs flux distributions have been produced in the past years: radio source counts at low frequency have been published even since the Sixties, while deep surveys at higher frequencies have been performed recently. Compilation of source counts can be found in several papers (see for example (Condon 1984), (Franceschini et al. 1989), (Toffolatti et al. 1998), (Windhorst et al. 1993)). Most of the data we used can be extracted from the references included in these papers.

We used the counts distributions at the frequencies between 150 and 8000 MHz, spanning a frequency range larger than the one covered by the TRIS experiment. In literature we found data at eight frequencies:  $\nu = 151$  MHz, 178 MHz, 408 MHz, 610 MHz, 1.4 GHz, 2.7 GHz, 5.0 GHz, 8.44 GHz. The complete list of the papers we examined is reported in Table 1. Some of those measurements were performed at a frequency slightly different from the nominal one. In this case, the original measurements were scaled to the nominal frequency by assuming a dependence of the source flux  $S(\nu) \sim \nu^{-0.7}$ . Usually the correction is negligible. The number counts extracted from Table 1 is shown in Figure 1.

## 3. Number counts distribution fit

The fit was performed on the differential number counts normalized to the Euclidean distribution of sources  $E(S) = S^{5/2}(dN/dS)$ , using the following analytical expression:

$$Q(S) = Q_1(S) + Q_2(S) = \frac{1}{A_1 S^{\varepsilon_1} + B_1 S^{\beta_1}} + \frac{1}{A_2 S^{\varepsilon_2} + B_2 S^{\beta_2}} \quad (2)$$

The best values of the fit parameters are summarized in Tables 2 and 3. This analytical fit function is empirical. It reproduces the distribution of the experimental data with some advantages: 1) it is a simple analytical function; 2) it allows to extend the extrapolation beyond the available data, because both the amplitude and slope of the tails are well defined, both at low and high fluxes; 3) it is built as the sum of two "populations" of sources with different emission, but similar behavior and shape; 4) the fitting procedure is independent on the source type and evolution but it is applied to the source counts as currently observed. In addition, this analytical form is simply a power law, with various indices at different values of flux, exactly as the observations suggest.

### 3.1. High flux distribution fit

To get the fit we first considered the source distribution at high fluxes (i.e. we evaluated the parameters of the component  $Q_1(S)$ ). For this high flux distribution we have data at all the considered frequencies. The best fit parameters are listed in Table 2. We found that the values of the spectral indices  $\varepsilon_1$  and  $\beta_1$  obtained at all the frequencies are very similar. We then decided to take a unique weighted average value for  $\varepsilon_1$  and  $\beta_1$ . The parameter  $\varepsilon_1$  is particularly well constrained by the data at 1400 MHz, where a large set of data with low scatter is available (see (White et al. 1997) and Figure 1). Conversely available data at 178 MHz do not span a flux range wide enough to constrain the two slopes.

Source counts at 2700 and 8440 MHz are the less accurate among the full data set we used. At both frequencies there are sets of data not completely overlapping and the statistics is poor. Therefore, to take into account these uncertainties, we assumed a uniform distribution of the parameter  $A_1$ . At  $\nu = 2700$  MHz we took  $A_1 = (6 - 12) \times 10^{-4}$ , while at  $\nu = 8440$  MHz we took  $A_1 = (16 - 34) \times 10^{-4}$  (see Table 2). In this fitting procedure we used all the data collected from the papers listed in the Table 1. We excluded from the fit only the seven data points at lowest flux published by White et al. (1997) at 1400 MHz because these data present a roll-off, exactly in the region where a changing of the slope is expected, but in the opposite direction. According to the authors, this roll-off is an indication of the incompleteness of the survey at the faint-flux limit.

### 3.2. Low flux distribution fit

We extended the fitting procedure to the counts at low flux, in order to constrain the distribution  $Q_2(S)$ . The two parameters  $A_2$  and  $\varepsilon_2$  fixed amplitude and slope of the low-flux tail of the distribution, while  $B_2$  and  $\beta_2$  are needed to fit the distribution in the region showing a change in the slope. Deep counts are available only at 0.61, 1.4, 5 and 8.44 GHz, but at 8.44 GHz the number of experimental points and their scatter do not allow to fit any parameter. In addition we considered the model of the low-flux tail published by Franceschini et al. (1989) at 1.4 and 5 GHz. This source evolution model fits the data also after the addition of the most recent measurements both at 1.4 and 5 GHz. The low-flux tail of the model compared with the experimental data and our fit  $Q(S)$  are shown in Figure 2. This evolution model is able to predict accurately the slope of the low-flux tail and we used it to get the value of  $\varepsilon_2$ , which is independent on the frequency (Franceschini 2007). The values of  $\varepsilon_2$ , obtained at 1.4 and 5 GHz, are fully compatible with the average value of  $\varepsilon_1$  previously evaluated. Combining the estimates at 1.4 and 5 GHz we get  $\varepsilon_2 = -0.856 \pm 0.021$ .

Since the model by Franceschini et al. (1989) is not able to fix the amplitude of the number counts, i.e. the parameter  $A_2$ , we evaluated this parameter by using the experimental data at 1.4 and 5 GHz. We get:  $A_2/A_1 = 0.24 \pm 0.02$  at 1.4 GHz;  $A_2/A_1 = 0.30 \pm 0.04$  at 5 GHz. The ratio  $A_2/A_1$  is almost independent on the frequency. The small change is due to the different contribution of the *flat-spectrum* sources in the total counts at the two frequencies in the low flux region (below  $10^{-5}$  Jy) and in the high flux region (10 mJy - 1 Jy).

Using the model of Franceschini et al. (1989) and Toffolatti et al. (1998) at 1.4, 5 and 8.4 GHz, we extrapolated the value of the ratio  $A_2/A_1$  also to the other frequencies. In order to evaluate  $A_2/A_1$  at lower frequencies we estimated the variation of  $A_2/A_1$  at 1.4 GHz excluding from the counts the *flat-spectrum* sources. This is the extreme condition, which holds at very low frequencies. In fact the other sources contributing to the number counts do not change significantly with frequency. We obtain in this situation that  $0.23 \leq A_2/A_1 \leq 0.24$ . The same result was obtained starting from data and model at 5 GHz. Therefore for the frequencies 151, 178, 408 and 610 MHz we take the value obtained at 1.4 GHz, but associating a larger error bar, due to the uncertainty in the extrapolation procedure:  $A_2/A_1 = 0.24 \pm 0.04$ .

We then evaluated the contribution of the *flat spectrum* sources in the total counts at 8.44 GHz (see Toffolatti et al. (1998)) in comparison with the counts at 5 GHz. In this way we estimate at 8.44 GHz the value  $A_2/A_1 = 0.31 \pm 0.04$ . At 2.7 GHz we took a value constrained by the results obtained at 1.4 and 5 GHz:  $A_2/A_1 = 0.24 - 0.30$ .

We finally estimated the  $B_2$  and  $\beta_2$ . They are important just to define the shape of the

distribution in the region showing a change in the slope. At 1.4 GHz data are accurate enough to constrain both parameters, but  $\beta_2$  can not be constrained at the other frequencies. Since the accuracy of these two parameters is not important for the calculation of the integrated brightness temperature, we assumed for them the average value for all the frequencies.

The summary of the best values of all the parameters of  $Q_2(S)$  is shown in Table 3. The number counts and the function which fit them are shown in Figure 1. In conclusion we can note that: 1)  $A_1$  and  $B_1$ , the two frequency dependent parameters of the fit, take different values at each frequency. The same is true for the ratio  $A_2/A_1$ . 2) The power law indices ( $\varepsilon_1$ ,  $\beta_1$ ,  $\varepsilon_2$  and  $\beta_2$ ) are frequency independent and we take a common value at all the frequencies.

## 4. The UERS contribution to the sky diffuse emission

### 4.1. Evaluation of the diffuse emission

The contribution of the UERS ( $B_{UERS}(\nu)$ ) to the sky brightness is evaluated by integrating the function  $S(dN/dS)$  from the largest flux ( $S_{max}$ ) of the measured sources down to the lowest fluxes ( $S_{min}$ ) corresponding to the faintest sources:

$$B_{UERS}(\nu) = \int_{S_{min}}^{S_{max}} \frac{dN}{dS}(\nu) \cdot S \, dS \quad (3)$$

The brightness temperature  $T_{UERS}(\nu)$  is by definition:

$$T_{UERS}(\nu) = B_{UERS}(\nu) \frac{\lambda^2}{2 k_B}, \quad (4)$$

$k_B$  being the Boltzmann constant. The values of  $T_{UERS}$  at the eight frequencies we considered are summarized in Table 4.

From the observations we have  $S_{max} \sim 10^2$  Jy (as measured at 151, 408 and 1400 MHz) and  $S_{min} \sim 10^{-6}$  Jy (as measured in the deepest counts at 5 GHz). While sources at higher fluxes if present in the surveyed sky region can be easily measured, the limit at low flux is set by the confusion limit or by the observation completeness. In other words there is no sharp limit at low flux in the population of the sources. We extended the integration down to very faint limits, several orders of magnitude below the faintest detected sources ( $S_{min} \sim 10^{-6}$  Jy). When the integration is extended down to  $S_{min} \sim 10^{-12}$  Jy the brightness

increase by 3 – 4 % and then the value converges. This increment is comparable with the total uncertainty we get on the value of the brightness, as shown in Figure 3.

We extended the integration also to higher values of the flux, in order to test also this integration limit. Increasing  $S_{max}$  well beyond the flux of the strongest sources observed, the integral change by less than 0.5% and quickly converges. This is a consequence of the very low statistics of sources at the highest fluxes. This is a confirmation that the large scale brightness is actually not sensitive to the upper limit of integration.

#### 4.2. Evaluation of the uncertainty

The error budget takes into account both the fit uncertainties and the number counts fluctuations over the observed sky region. The fit uncertainties were evaluated by means of Monte Carlo simulations. For each parameter we considered a gaussian distribution with standard deviation as reported in Tables 2 and 3. Only for the values of  $A_1$  at 2.7 and 8.44 GHz and for  $A_2/A_1$  at 2.7 GHz we assumed a uniform distribution inside the interval reported in Tables 2 and 3. The error bars of the parameters of the fit (in particular  $A_2/A_1$  and  $\varepsilon_2$ ) include the uncertainty on the extrapolation at the lowest fluxes for the various frequencies. We underline that, as shown in Figure 3, the contribution to the brightness temperature of the low-flux tail (below  $\sim 10^{-6}$  Jy) is lower than the overall uncertainty reported in Table 4.

The statistical fluctuations of the sources' number counts have no effect in a large part of the distribution because the number of sources is quite large. We concentrated on the effect of the fluctuation of the few sources with the highest flux. We considered these sources randomly distributed and therefore their fluctuation is Poissonian. We evaluated the fluctuation of the brightness in a patch of the sky corresponding to the beam of TRIS:  $\Omega_{TRIS} \sim 0.1$  sr. The upper limit of the contribution to the temperature uncertainty due to the fluctuation in the number of sources is directly measured by the maximum of the function

$$C(S_{min}) = \frac{\lambda^2}{2k_B\Omega_{TRIS}} \frac{\int_{S_{min}}^{100Jy} \frac{dN}{dS} S dS}{\int_{S_{min}}^{100Jy} \frac{dN}{dS} dS} \quad (5)$$

plotted in Figure 4 for the specific case of the 1400 MHz data. For all the frequencies this maximum falls around  $\sim 5$  Jy, and its value is from 2 to 6 times smaller than the corresponding values reported in Table 4. Therefore for every frequency, and over the full flux range, the error of the brightness temperature is dominated by the statistical uncertainties of the fit parameters.



The relative error bar of the brightness temperature is 6 – 7% at 151, 408, 610 and 1400 MHz increasing up to 9% at 5000 MHz. At 178 MHz the available measurements are few and old and the obtained error bar is 13%. At 2700 and 8440 MHz both the quantity and the quality of the data do not allow accurate estimates of the parameters of the fit and we get an uncertainty of 25 – 30%.

### 4.3. Frequency dependence

The integrated contribution of the UERS to the brightness of the sky at the various frequencies is shown in Figure 5. The distribution can be fitted by a power law:

$$T_{UERS}(\nu) = T_0 \left( \frac{\nu}{\nu_0} \right)^{\gamma_0} \quad (6)$$

Setting  $\nu_0 = 610$  MHz (chosen because it is close to one of the channels of the TRIS experiment), we obtain the best fit of  $T_0$  and  $\gamma_0$  shown in Table 5 (*FIT1*). As shown in Figure 5, in spite of the large error bars at 2700 and 8440 MHz, scatter of the data points is limited. The fit of a single power law, done excluding the data with the largest uncertainty (at  $\nu = 178$ , 2700 and 8440 MHz), gives the values of  $T_0$  and  $\gamma_0$  shown in Table 5 (*FIT2*). Now the scatter of the experimental data is much smaller, as shown by the value of the reduced  $\chi^2$ .

In both cases the results obtained are fully compatible with the slope of the *steep spectrum* sources, which are therefore the main contributors to the source counts. However it is interesting to check the contribution of the *flat spectrum* sources especially at high frequencies. We assumed a *flat spectrum* component with fixed slope  $\gamma_1 = -2.00$  and a dominant *steep spectrum* component with slope  $\gamma_0 = -2.70$ :

$$T_{UERS}(\nu) = T_0 \left( \frac{\nu}{\nu_0} \right)^{\gamma_0} + T_1 \left( \frac{\nu}{\nu_0} \right)^{\gamma_1} \quad (7)$$

The results of the fit of  $T_0$  and  $T_1$  are shown in Table 5 (*FIT3*). Doing so we can get an estimate of the contribution of the *flat-spectrum* component in the number counts at the various frequencies. The value of  $T_{UERS}(\nu)(\nu/\nu_0)^{2.70}$  at the frequencies analyzed is shown in Figure 6, together with the power law best fits. Figure 6 shows that the two last fits (*FIT2* and *FIT3*) are equivalent within the error bars.

## 5. Discussion

### 5.1. Analytical form of the fit function

As discussed in Section 3, the fit function  $Q(S)$  is a power law distribution taking different slopes and amplitudes in three different regions of the sources' flux. We prefer to deal with a power law (like  $Q(S)$ ) instead of a polynomial fit, as performed by Katgert et al. (1988) and Hopkins et al. (2003). A polynomial fit can be better adapted to the experimental points, but its validity range is restricted to the region covered by experimental points. Therefore it is not possible to use a polynomial fit to extrapolate the distribution outside this range. Conversely our fit function can be extrapolated because amplitude and slope of the tails are well defined and take into account the shapes expected from the counts evolution models (Franceschini et al. 1989).

According to Longair (1978) we should expect a broadened maximum in the distribution of the source counts with increasing frequency. This indication seems to be confirmed looking at the differential counts shown in ((Kellermann & Wall 1987) and (Condon 1984)). In spite of these expectations we have obtained a good fit of the counts at the various frequencies, using the same function with the same slopes, as shown Figure 1. Part of this effect is probably hidden by the larger scatter of the high frequency differential counts. In any case the broadening of the maximum could be marginally observed above 1400 MHz and the effect is not relevant for the calculation of the contribution to the sky brightness.

### 5.2. Frequency dependence

The spectral dependence of the brightness temperature  $T_{UERS}$  follows the expectations at low frequency where the number counts are dominated by the sources with steep spectrum:  $\alpha \sim 0.7$ . At high frequency the situation is more complex. We could expect a flattening, because at these frequencies the number counts of *flat-spectrum* sources begin to be important. It will probably appear at frequencies higher than 1400 MHz. Unfortunately the available data are not accurate enough to constrain the fit parameters (in particular  $A_1$ ) at 2700 and 8440 MHz. The values obtained at these two frequencies, lower than the values expected looking at the other frequencies, could also be an indication of incompleteness of the surveys (see Figure 6). Conversely at 5000 MHz data are better and numerous. We obtain a value for  $T_{UERS}$  fully consistent with the slope of the data at low frequency, where *steep-spectrum* sources are dominating, even if there is a marginal indication of a spectral flattening (see Figure 6). In fact when we fit the data adding the contribution of the *flat-spectrum* sources we get an estimate of this contribution which is  $T_1/T_0 \simeq 2\%$  at  $\nu = 610$  MHz and  $T_1/T_0 \simeq 9\%$

at  $\nu = 5$  GHz (see *FIT3* in the Table 5).

### 5.3. Previous estimates of $T_{UERS}$

The values of brightness temperature shown in Table 4 have error bars of roughly 7% at most frequencies. The uncertainty is a bit larger at 178 MHz and even worse at 2700 and 8440 MHz, because of the quality of the number counts data. So far very few estimates of  $T_{UERS}$  have been published (see (Longair 1966), (Wall 1990) and (Burigana et al. 2004)), and the frequencies covered were limited and sometimes the uncertainty was not quoted. Our results are in agreement with the values previously estimated by Longair (1966),  $T_{UERS}(178 \text{ MHz}) = 23 \pm 5$  K, and by Wall (1990),  $T_{UERS}(408 \text{ MHz}) \simeq 2.6$  K,  $T_{UERS}(1.4 \text{ GHz}) \simeq 0.09$  K, and  $T_{UERS}(2.5 \text{ GHz}) \simeq 0.02$  K, but our error bars are definitely smaller. The accuracy of the estimated values of  $T_{UERS}$  is particularly important if this contribution is to be subtracted to calculate the value of the CMB temperature at low frequency. Table 4 suggests that the value of  $T_{UERS}$  needs to be accurately evaluated up to a frequency of several GHz, because its value is not negligible.

## 6. Conclusions

We used the source number - flux measurements in literature to evaluate the contribution of the Unresolved Extragalactic Radio Sources to the diffuse brightness of the sky. We analyzed the count distributions at eight frequencies between 150 and 8000 MHz, spanning over the frequency range partially covered by the TRIS experiment (see (Zannoni et al. 2007)):  $\nu = 151$  MHz, 178 MHz, 408 MHz, 610 MHz, 1.4 GHz, 2.7 GHz, 5.0 GHz, 8.44 GHz.

We optimized the fitting function of the experimental number counts distribution. The differential number counts ( $dN/dS$ ) at the various frequencies are well described by a multi power law empirical distribution  $Q(S)$  (see Equation 2). The amplitudes ( $A_1$  and  $B_1$ ) are frequency dependent parameters of the fit and have different values at each frequency. Conversely the power law indices ( $\varepsilon_1$ ,  $\beta_1$ ,  $\varepsilon_2$  and  $\beta_2$ ) have a common value at all the frequencies.

The contribution of the UERS to the sky brightness was evaluated by integrating the function  $S(dN/dS)$  from the largest flux ( $S_{max} = 10^2$ ) of the measured sources down to the lowest fluxes ( $S_{min} = 10^{-12}$ ) corresponding to the expected faintest sources. We got the brightness temperature with a relative error bar of  $\delta T_{UERS}/T_{UERS} \simeq 6 - 7\%$  at  $\nu = 151$ , 408, 610 and 1400 MHz,  $\delta T_{UERS}/T_{UERS} \simeq 9\%$  at  $\nu = 5000$  MHz,  $\delta T_{UERS}/T_{UERS} \simeq 13\%$  at  $\nu = 178$  MHz and  $\delta T_{UERS}/T_{UERS} \simeq 25 - 30\%$  at  $\nu = 2700$  and 8440 MHz.

We finally evaluated the spectral dependence of the point source integrated brightness. As expected this dependence can be described using a power law with a spectral index  $\gamma_0 \simeq -2.7$ , in agreement with the frequency dependence of the flux emitted by the *steep-spectrum* sources. We have also tested the contribution of the *flat-spectrum* sources, adding a second component with the slope  $\gamma_1 = -2.0$ . The contribution of these sources starts to be relevant only at frequencies above several GHz. In fact we estimated a contribution by *flat-spectrum* sources  $\sim 2\%$  at 610 MHz and  $\sim 9\%$  at 5 GHz.

The above results were used to evaluate the CMB temperature at frequencies close to 1 GHz from absolute measurements of the sky temperature made by our group (see (Zannoni et al. 2007), (Gervasi et al. 2007), (Tartari et al. 2007)).

**Acknowledgements:** This work is part of the TRIS activity, which has been supported by MIUR (Italian Ministry of University and Research), CNR (Italian National Council of Research) and the Universities of Milano and of Milano-Bicocca. The authors acknowledge A. Franceschini for useful discussions and the anonymous referee for helpful comments to the draft.

## REFERENCES

- Aizu, K., Inoue, M., Tabara, H., and Kato, T., 1987, *IAU Symp.*, **124**, 565-568.
- Baldwin, J.E., Boysen, R.C., Hales, S.E.G., Jennings, J.E., Waggett, P.C., Warner, P.J., and Wilson, D.M.A., 1985, *MNRAS*, **217**, 717-730.
- Bennett, C.L., Lawrence, C.R., Garcia-Barreto, J.A., Hewitt, J.N., and Burke, B.F., 1983, *Nature*, **301**, 686-688.
- Birkinshaw, M., 1986, *MNRAS*, **222**, 731-751.
- Bondi, M., Ciliegi, P., Zamorani, G., Gregorini, L., Vettolani, G., Parma, P., de Ruiter, H., Le Fèvre, O., Arnaboldi, M., Guzzo, L., Maccagni, D., Scaramella, R., Adami, C., Bardelli, S., Bolzonella, M., Bottini, D., Cappi, A., Foucaud, S., Franzetti, P., Garilli, B., Gwyn, S., Ilbert, O., Iovino, A., Le Brun, V., Marano, B., Marinoni, C., McCracken, H.J., Meneux, B., Pollo, A., Pozzetti, L., Radovich, M., Ripepi, V., Rizzo, D., Scoddeggio, M., Tresse, L., Zanichelli A., Zucca, E., 2003, *A&A*, **403**, 857-867.
- Bondi, M., Ciliegi, P., Venturi, T., Dallacasa, D., Bardelli, S., Zucca, E., Athreya, R.M., Gregorini, L., Zanichelli A., Le Fèvre, O., Contini, T., Garilli, B., Iovino, A., Temporin, S., Vergani, D., 2007, *A&A*, **463**, 519-527.
- Burigana, C., De Zotti, G., and Feretti, L., 2004, *New A Rev.*, **48**, 1107-1117.
- Ciliegi, P., Zamorani, G., Hasinger, G., Lehmann, I., Szokoly, G., and Wilson, G., 2003, *A&A*, **398**, 901-918.
- Coleman, P.H., Condon, J.J., and Hazard, C., 1985, *AJ*, **90**, 1437-1445.
- Colla, G., Fanti, C., Fanti, R., Ficarra, A., Formiggini, L., Gandolfi, E., Gioia, I., Lari, C., Marano, B., Padrielli, L., Tomasi, P., 1973, *A&A Suppl. Ser.*, **11**, 291-325.
- Condon, J.J., Condon, M.A., Hazard, C., 1982, *AJ*, **87**, 739-750.
- Condon, J.J., and Mitchell, K.J., 1982, *AJ*, **87**, 1429-1437.
- Condon, J.J., 1984, *ApJ*, **287**, 461-474.
- Condon, J.J., and Mitchell, K.J., 1984, *AJ*, **89**, 610-617.
- Danese, L., De Zotti, G., Franceschini, A., Toffolatti, L., 1987, *ApJ*, **318**, L15-L20.
- Davis, M.M., 1971, *AJ*, **76**, 980-992.

- Fixen, D.J., Cheng, E.S., Gales, J.M., Mather, J.C., Shafer, R.A., and Wright, E.L., 1996, *ApJ*, **473**, 576-587.
- Fomalont, E.B., Bridle, A.H., and Davis, M.M., 1974, *A&A*, **36**, 273-278.
- Fomalont, E.B., Kellermann, K.I., Wall, J.V., and Weistrop, D., 1984, *Science*, **225**, 23-28.
- Fomalont, E.B., Kellermann, K.I., Anderson, M.C., Weistrop, D., Wall, J.V., Windhorst, R.A., and Kristian, J.A., 1988, *AJ*, **96**, 1187-1191.
- Fomalont, E.B., Kellermann, K.I., Partridge, R.B., Windhorst, R.A., and Richards, E.A., 2002, *AJ*, **123**, 2402-2416.
- Franceschini, A., Toffolatti, L., Danese, L., and De Zotti, G., 1989, *ApJ*, **344**, 35-45.
- Franceschini, A., 2007, private communication.
- Gervasi, M., Tartari, A., Zannoni, M., Boella, G., and Sironi, G., 2007, *ApJ*, submitted.
- Gower, I.F.R., 1966, *MNRAS*, **133**, 151-161.
- Grueff, G., 1988, *A&A*, **193**, 40-46.
- Gruppioni, C., Zamorani, G., de Ruiter, H.R., Parma, P., Mignoli, M., and Lari, C., 1997, *MNRAS*, **286**, 470-482.
- Hales, S.E.G., Baldwin, J.E., and Warner, P.J., 1988, *MNRAS*, **234**, 919-936.
- Hopkins, A.M., Afonso, J., Chan, B., Cram, L.E., Georgakakis, A., and Mobasher, B., 2003, *AJ*, **125**, 465-477.
- Katgert, P., Katgert-Merkelijn, J.K., Le Poole, R.S., and van der Laan, H., 1973, *A&A*, **23**, 171-194.
- Katgert, J.K., Spinrad, H., 1974, *A&A*, **35**, 393-406.
- Katgert, P., 1976, *A&A*, **49**, 221-234.
- Katgert, P., 1979, *A&A*, **73**, 107-112.
- Katgert, P., Oort, M.J.A., and Windhorst, 1988, *A&A*, **195**, 21-24.
- Katgert-Merkelijn, J.K., Robertson, J.G., Windhorst, R.A., and Katgert, P., 1985, *A&A Suppl. Ser.*, **61**, 517-535.

- Kellermann, K.I. and Wall, J.V., 1987, *IAU Symp.*, **124**, 545-564.
- Ledden, J.E., Broderick, J.J., Condon, J.J., and Brown, R.L., 1980, *AJ*, **85**, 780-788.
- Longair, M.S., 1966, *MNRAS*, **133**, 421-436.
- Longair, M.S., 1978, in *Observational Cosmology - 8th Advanced Course Swiss Society of Astronomy and Astrophysics*, 172-257.
- Machalski, J., 1978, *A&A*, **65**, 157-164.
- McGilchrist, M.M., Baldwin, J.E., Riley, J.M., Titterton, D.J., Waldram, E.M., and Warner, P.J., 1990, *MNRAS*, **246**, 110-122.
- Mills, B.Y., Davies, I.M., and Robertson, J.G., 1973, *Aust. J. Phys.*, **26**, 417-425.
- Owen, F.N., Condon, J.J., and Ledden, J.E., 1983, *AJ*, **88**, 1-15.
- Partridge, R.B., Hildrup, K.C., and Ratner, M.I., 1986, *ApJ*, **308**, 46-52.
- Pauliny-Toth, I.I.K., Witzel, A., Preuss, E., Kuhr, H., Kellermann, K.I., Fomalont, E.B., and Davis, M.M., 1978, *AJ*, **83**, 451-474.
- Pauliny-Toth, I.I.K., Steppe, H., and Witzel, A., 1980, *A&A*, **85**, 329-331.
- Peacock, J.A., and Gull, S.F., 1981, *MNRAS*, **196**, 611-633.
- Peacock, J.A., and Wall, J.V., 1981, *MNRAS*, **194**, 331-349.
- Pearson, T.J., and Kus, A.J., 1978, *MNRAS*, **182**, 273-274.
- Prandoni, I., Gregorini, L., Parma, P., de Ruiter, H.R., Vettolani, G., Wieringa, M.H., and Ekers, R.D., 2001, *A&A*, **365**, 392-399.
- Prandoni, I., Parma, P., Wieringa, M.H., de Ruiter, H.R., Gregorini, L., Mignano, A., Vettolani, G., and Ekers, R.D., 2006, *A&A*, **457**, 517-529.
- Richards, E.A., 2000, *ApJ*, **533**, 611-630.
- Seielstad, G.A., 1987, *PASP*, **95**, 32-34.
- Shaver, P.A., and Pierre, M., 1989, *A&A*, **220**, 35-41.
- Sironi, G., Limon, M., Marcellino, G., Bonelli, G., Bersanelli, M., Conti, G. and Reif, K., 1990, *ApJ*, **357**, 301-308.

- Tartari, A., Zannoni, M., Gervasi, M., Boella, G., and Sironi, G., 2007, *ApJ*, submitted.
- Toffolatti, L., Argueso Gomez, F., De Zotti, G., Mazzei, P., Franceschini, A., Danese, L., and Burigana, C., 1998, *MNRAS*, **297**, 117-127.
- Vallée, J.P., and Roger, R.S., 1989, *A&A Suppl. Ser.*, **77**, 31-38.
- White, R.L., Becker, R.H., Helfand, D.J., and Gregg, M.D., 1997, *ApJ*, **475**, 479-493.
- Wall, J.V., Pearson, T.J., and Longair, M.S., 1980, *MNRAS*, **193**, 683-706.
- Wall, J.V., Pearson, T.J., and Longair, M.S., 1981, *MNRAS*, **196**, 597-610.
- Wall, J.V., and Peacock, J.A., 1985, *MNRAS*, **216**, 173-192.
- Wall, J.V., 1990, *IAU Symposium*, **139**, 327-332.
- Webster, A., 1977, *IAU Symposium*, **74**, 75-81.
- Wilson, A.S., and Vallée, J.P., 1982, *A&A Suppl. Ser.*, **47**, 601-609.
- Windhorst, R.A., Miley, G.K., Owen, F.N., Kron, R.G., and Koo, D.C., 1985, *ApJ*, **289**, 494-513.
- Windhorst, R.A., Fomalont, E.B., Partridge, R.B., and Lowenthal, J.D., 1993, *ApJ*, **405**, 498-517.
- Zannoni, M., Tartari, A., Gervasi, M., De Lucia, A., Passerini A., Cavaliere, F., Boella, G., and Sironi, G., 2007, *ApJ*, submitted.



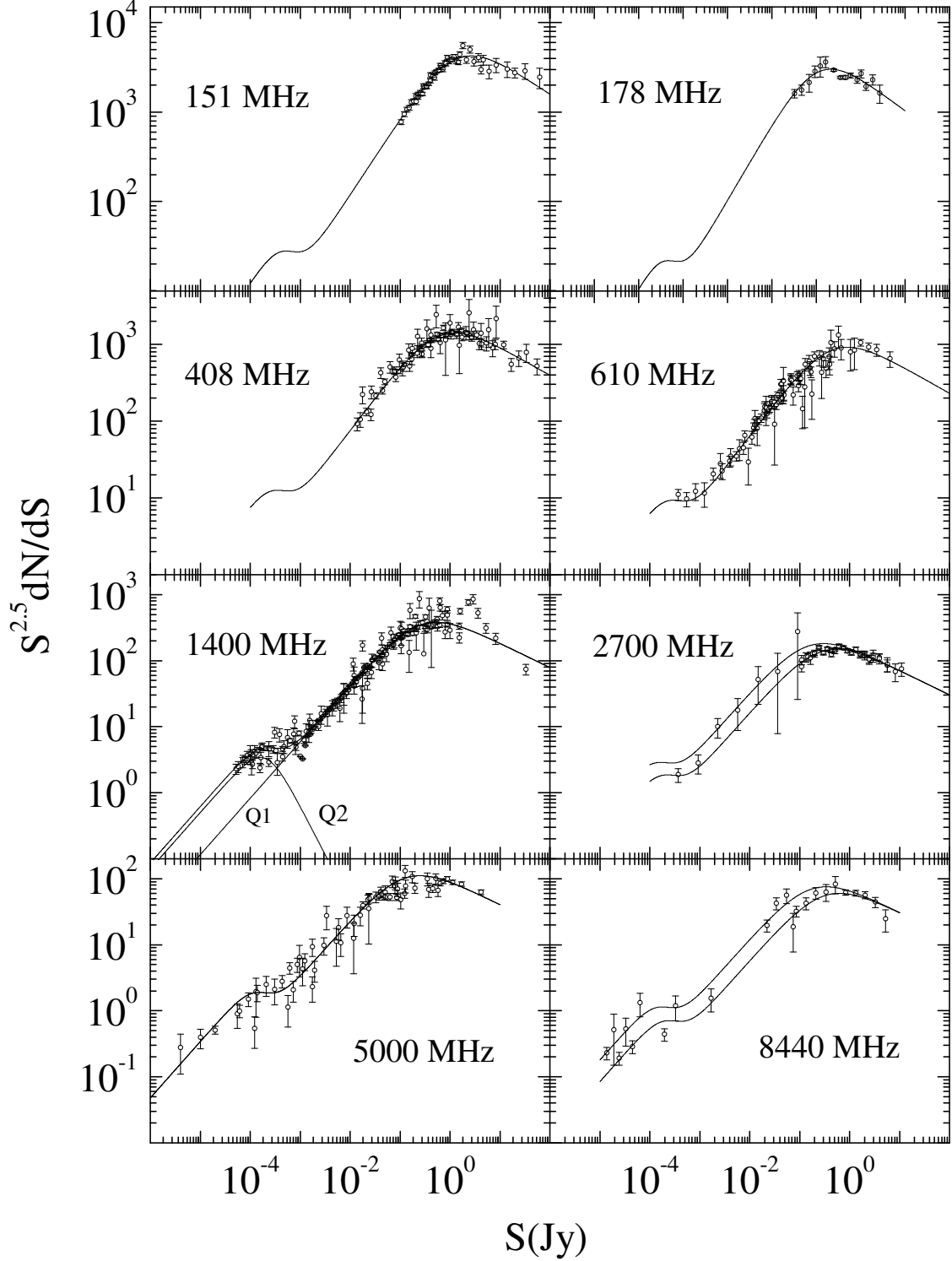


Fig. 1.— Data and fit ( $Q(S)$ ) of source counts at the various frequencies. Data are extracted from papers listed in Table 1. At  $\nu = 1.4$  GHz the two terms  $Q_1$  and  $Q_2$  of the fit are also shown. At  $\nu = 2.7$  and  $\nu = 8.44$  GHz the fit profiles are obtained using the distribution limits of  $A_1$  reported in Table 2.

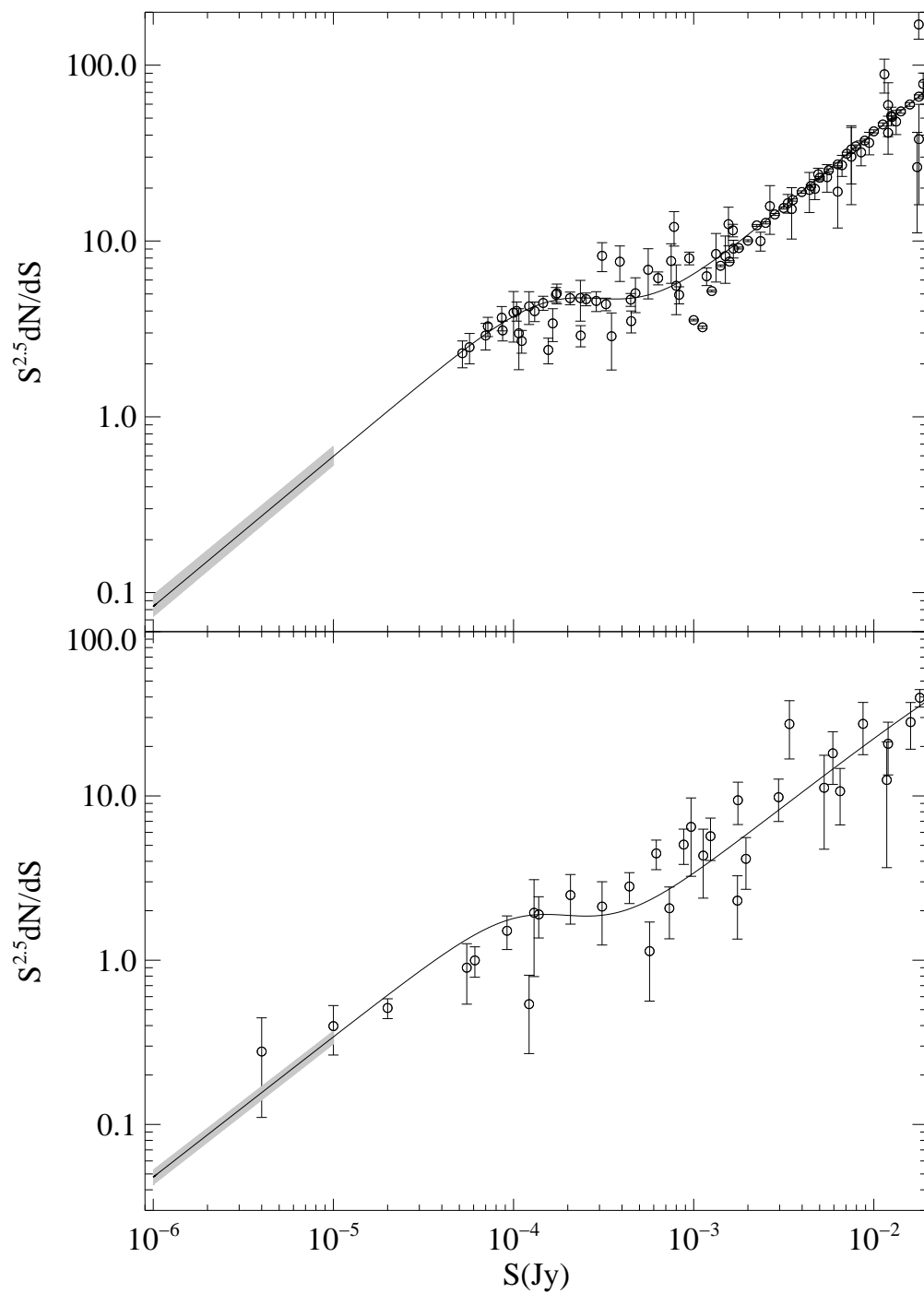


Fig. 2.— Data and fit of source counts at  $\nu = 1.4$  and at  $\nu = 5$  GHz. The low-flux tail of the model by Franceschini et al. (1989) is also shown (grey region). The thickness is an indication of the uncertainty in the normalization with the experimental data.

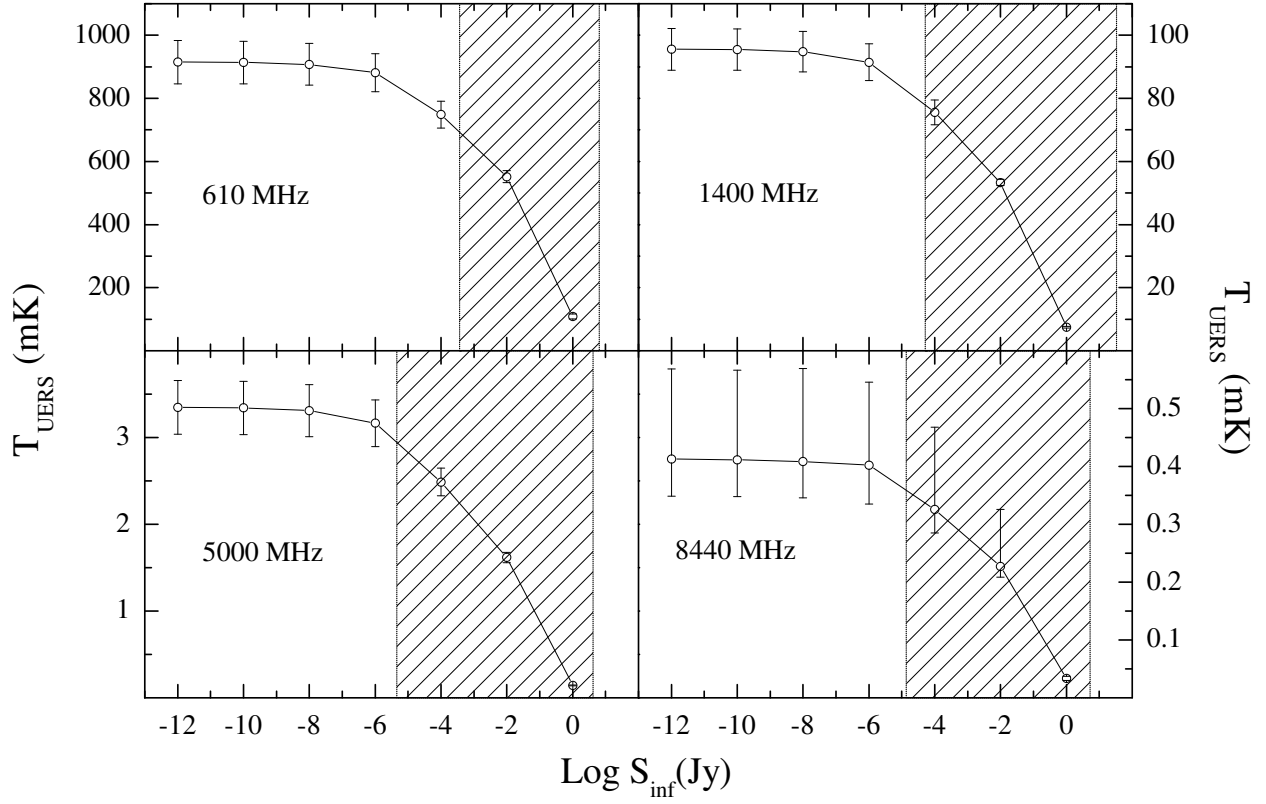


Fig. 3.— The integrated brightness temperature at selected frequencies is shown *vs* the lowest flux value of source counts ( $S_{\text{inf}}$ ). The upper limit of the integration is fixed at 100 Jy. The region where experimental data are available is also shown (shaded region).

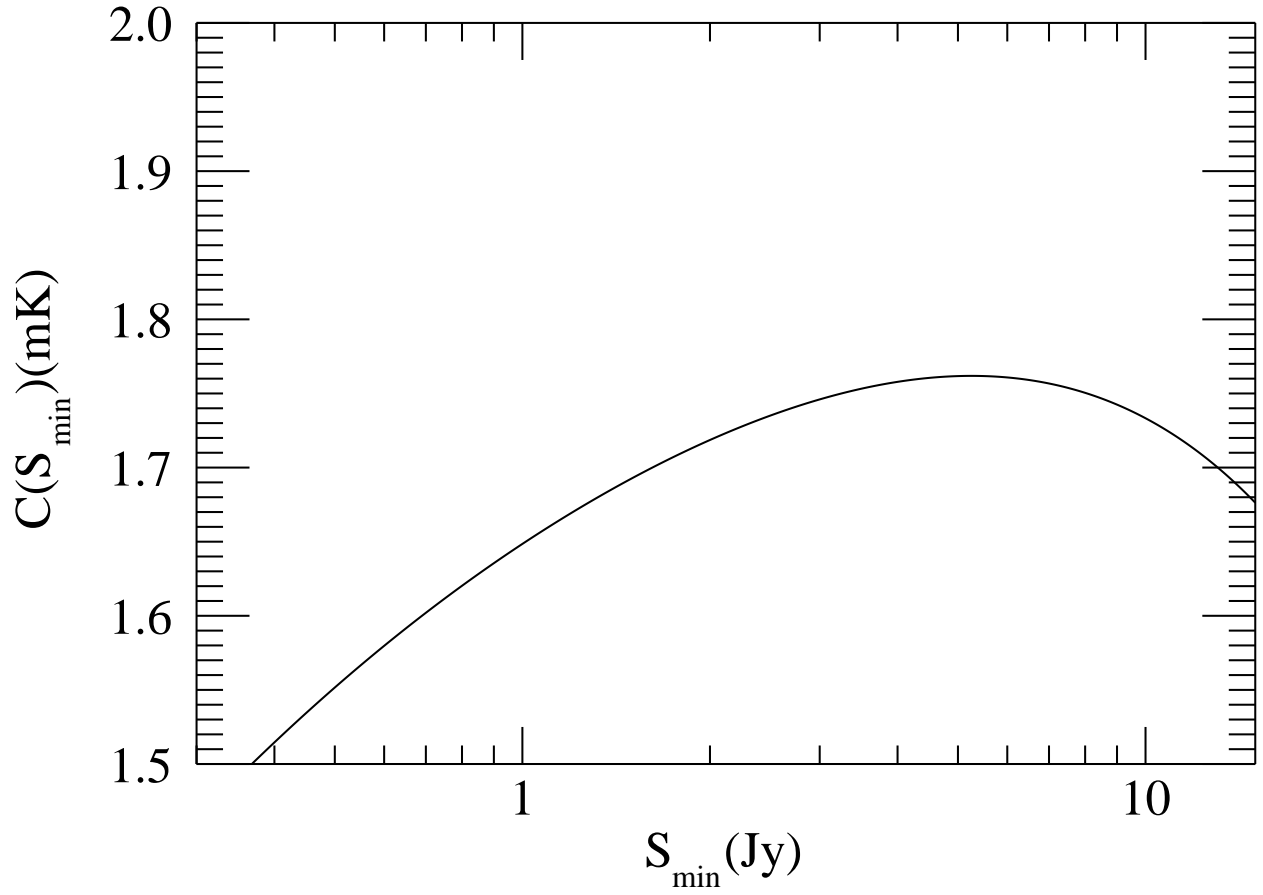


Fig. 4.— Frequency: 1400 MHz. The maximum of the plotted function  $C(S_{\min})$  vs  $S_{\min}$  sets an upper limit to the contribution of the source number fluctuation to the brightness temperature uncertainty in a beam large 0.1 sr (see the text).

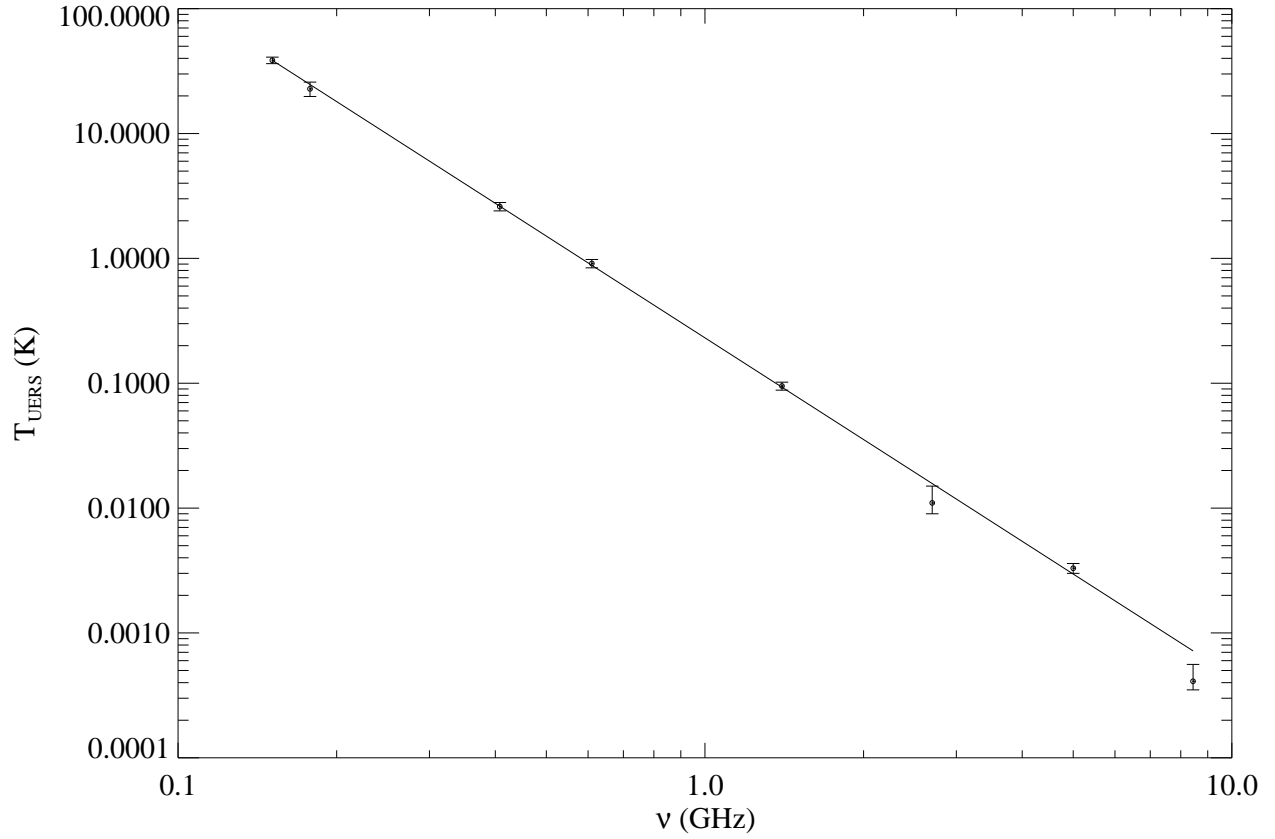


Fig. 5.— Frequency spectrum of the brightness temperature of the unresolved extragalactic radio sources. The continuous line is *FIT1* (see the text).

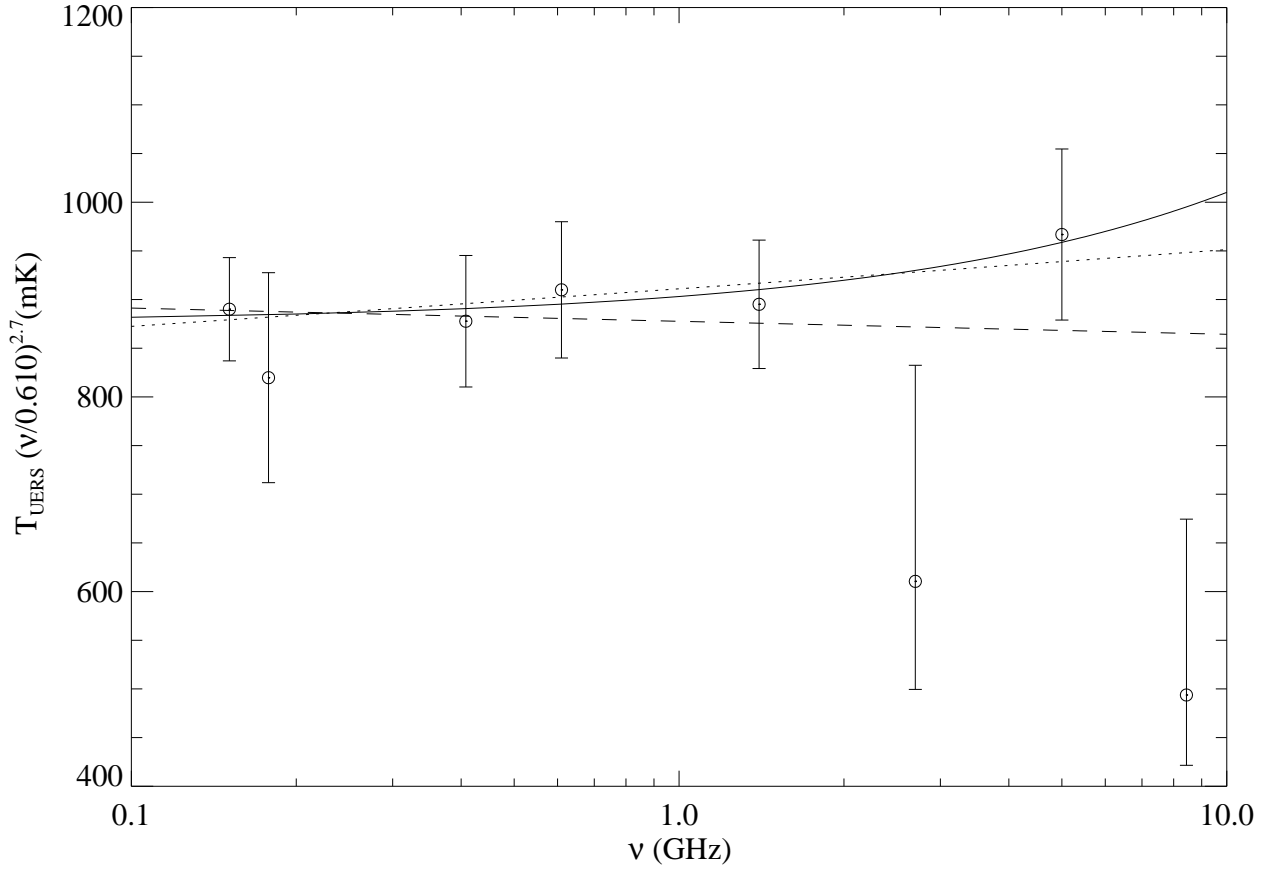


Fig. 6.— Brightness temperature of the extragalactic radio sources. The values are multiplied by the power law  $(\nu/0.61GHz)^{2.70}$ . The fit curves discussed in the text are also shown: *FIT1* (dashes); *FIT2* (dots); *FIT3* (continuous line).

Table 1. Reference papers for the extragalactic radio source counts.

Frequency	Reference
151 MHz	Baldwin et al. (1985), Hales et al. (1988), McGilchrist et al. (1990).
178 MHz	Gower (1966), Longair (1966).
408 MHz	Condon (1984), Colla et al. (1973), Mills et al. (1973), Pearson & Kus (1978), Wall et al. (1980), Birkinshaw (1986), Grueff (1988), Vallée & Roger (1989).
610 MHz	Condon (1984), Wilson & Vallée (1982), Katgert-Merkelijn et al. (1985), Katgert (1979), Bondi et al. (2007).
1.4 GHz	Franceschini et al. (1989), Katgert et al. (1973), Katgert & Spinrad (1974), Katgert (1976), Fomalont et al. (1974), Machalski (1978), Bondi et al. (2003), Condon et al. (1982), Condon & Mitchell (1982), Coleman et al. (1985), Condon & Mitchell (1984), Windhorst et al. (1985), White et al. (1997), Richards (2000), Prandoni et al. (2001), Hopkins et al. (2003).
2.7 GHz	Peacock & Wall (1981), Wall et al. (1981), Wall & Peacock (1985), Gruppioni et al. (1997).
5 GHz	Franceschini et al. (1989), Partridge et al. (1986), Pauliny-Toth et al. (1980), Owen et al. (1983), Davis (1971), Bennett et al. (1983), Ledden et al. (1980), Fomalont et al. (1984), Pauliny-Toth et al. (1978), Fomalont et al. (1988), Prandoni et al. (2006), Ciliegi et al. (2003).
8.44 GHz	Toffolatti et al. (1998), Windhorst et al. (1993), Aizu et al. (1987), Seielstad (1983), Fomalont et al. (2002).

Table 2. Estimated values of the parameters of the fit function  $Q_1(S)$ :  $\varepsilon_1$ ,  $\beta_1$ ,  $A_1$  and  $B_1$ .

Frequency (MHz)	Parameter		Parameter	
	$\varepsilon_1$	$\beta_1$	$A_1(\times 10^{-4})$	$B_1(\times 10^{-4})$
151	$-0.95 \pm 0.05$	$0.37 \pm 0.06$	$1.65 \pm 0.02$	$1.14 \pm 0.04$
178	...	$0.31 \pm 0.04^a$	$1.9 \pm 0.3$	$1.75 \pm 0.07$
408	$-0.84 \pm 0.03$	$0.38 \pm 0.04$	$2.60 \pm 0.05$	$4.6 \pm 0.1$
610	$-0.91 \pm 0.07$	$0.4 \pm 0.1$	$3.04 \pm 0.08$	$7.9 \pm 0.6$
1400	$-0.854 \pm 0.007$	$0.37 \pm 0.02$	$4.65 \pm 0.02$	$23.2 \pm 0.8$
2700	$-0.76 \pm 0.04$	$0.37 \pm 0.06$	6 – 12	$60 \pm 2$
5000	$-0.83 \pm 0.05$	$0.29 \pm 0.06$	$8.4 \pm 0.4$	$105 \pm 4$
8440	$-0.78 \pm 0.05$	$0.47 \pm 0.15$	16 – 34	$138 \pm 9$
W.Av.	$-0.854 \pm 0.007$	$0.37 \pm 0.02$	...	...

<sup>a</sup>The value of  $\beta_1$  at 178 MHz has been evaluated using only few data and for this reason it is not included in the calculation of the average value.



Table 3. Estimated values of the parameters of the fit function  $Q_2(S)$ :  $\varepsilon_2$ ,  $\beta_2$ ,  $A_2/A_1$  and  $B_2/B_1$ .

Frequency (MHz)	Parameter		Parameter	
	$\varepsilon_2$	$\beta_2$	$A_2/A_1$	$B_2/B_1(\times 10^7)$
151	...	...	$0.24 \pm 0.04^a$	...
178	...	...	$0.24 \pm 0.04^a$	...
408	...	...	$0.24 \pm 0.04^a$	...
610	...	...	$0.24 \pm 0.04^a$	$1.14 \pm 0.4$
1400	$-0.862 \pm 0.032^a$	$1.47 \pm 0.15$	$0.24 \pm 0.02$	$1.9 \pm 0.2$
2700	...	...	$0.24 - 0.30$	...
5000	$-0.852 \pm 0.027^a$	...	$0.30 \pm 0.04$	$2.3 \pm 1$
8440	...	...	$0.31 \pm 0.04^b$	...
W.Av.	$-0.856 \pm 0.021$	$1.47 \pm 0.15$	...	$1.8 \pm 0.2$

<sup>a</sup>Parameter estimated by using the model by Franceschini et al. (1989).

<sup>b</sup>Parameter estimated by using the model by Toffolatti et al. (1998).

Table 4. Brightness temperature of the unresolved extragalactic radio sources.

Frequency (MHz)	$T_{uers}$ (mK)	$\Delta T_{uers}$ (mK)
151	38600	2300
178	22800	3000
408	2600	200
610	910	70
1400	95	7
2700	11	$\begin{smallmatrix} +4 \\ -2 \end{smallmatrix}$
5000	3.3	0.3
8440	0.41	$\begin{smallmatrix} +0.15 \\ -0.06 \end{smallmatrix}$

Table 5. Frequency dependence of the brightness temperature of the unresolved extragalactic radio sources (see the text).

	FIT1 <sup>a</sup>	FIT2 <sup>b</sup>	FIT3 <sup>c</sup>
$\nu_0$ (MHz)	610	610	610
$T_0$ (mK)	$880 \pm 28$	$903 \pm 30$	$876 \pm 22$
$\gamma_0$	$-2.707 \pm 0.027$	$-2.681 \pm 0.029$	-2.70
$T_1$ (mK)	...	...	$18.9 \pm 0.2$
$\gamma_1$	...	...	-2.00
$\chi_R^2$	1.26	0.11	0.05
$Q$	0.026	0.0095	0.0031

<sup>a</sup>*FIT1* has been obtained using all the experimental data and fitting a single power law.

<sup>b</sup>*FIT2* has been obtained excluding the experimental data at  $\nu = 178$  MHz, 2.7 GHz, 8.44 GHz and fitting a single power law.

<sup>c</sup>*FIT3* has been obtained excluding the experimental data at  $\nu = 178$  MHz, 2.7 GHz, 8.44 GHz and fitting *steep-spectrum* plus *flat-spectrum* sources.